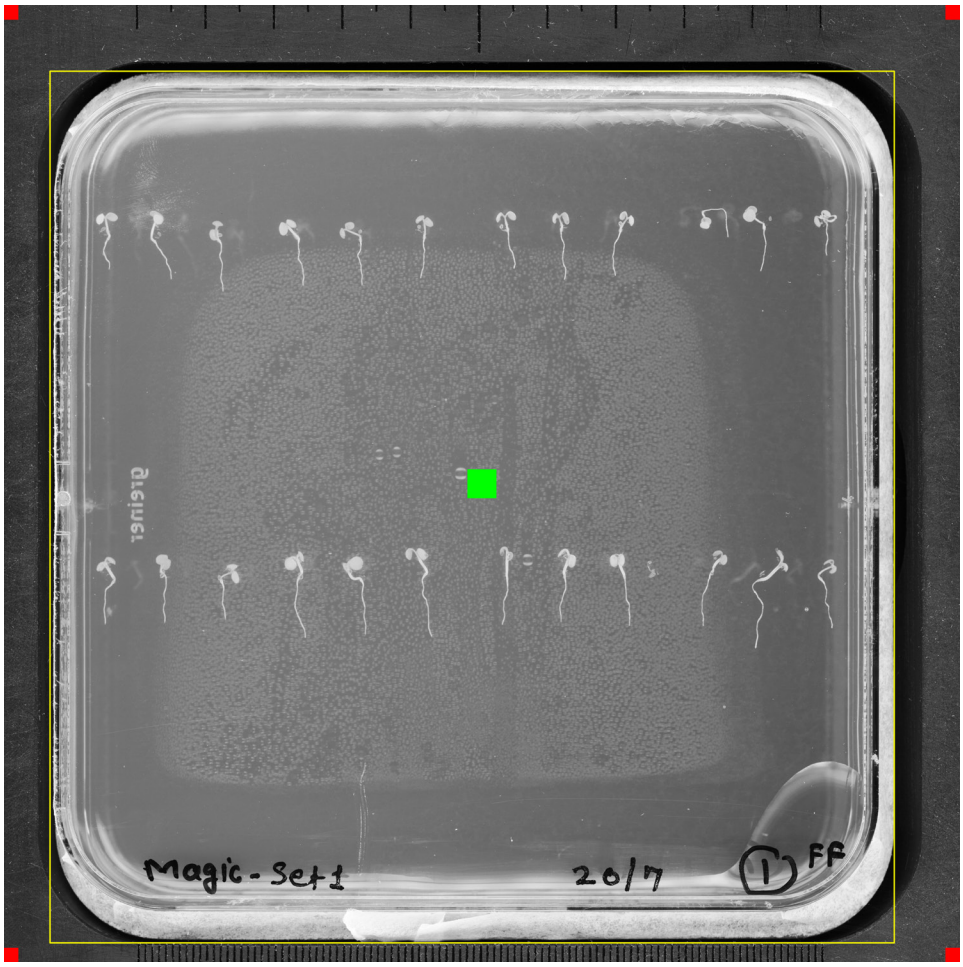

Supplemental Figure 1. Detection of the plate's area

A greyscale representation of the original image is used to detect the plate area. Areas at the corners (red squares) and center of the image (green square) are used to calculate the upper and lower threshold value. Due to the rounded corners of the used plate, this method would succeed even if the image was cropped by the user before supplying it to the pipeline. The detected region of interest (ROI) is shown as yellow rectangle.

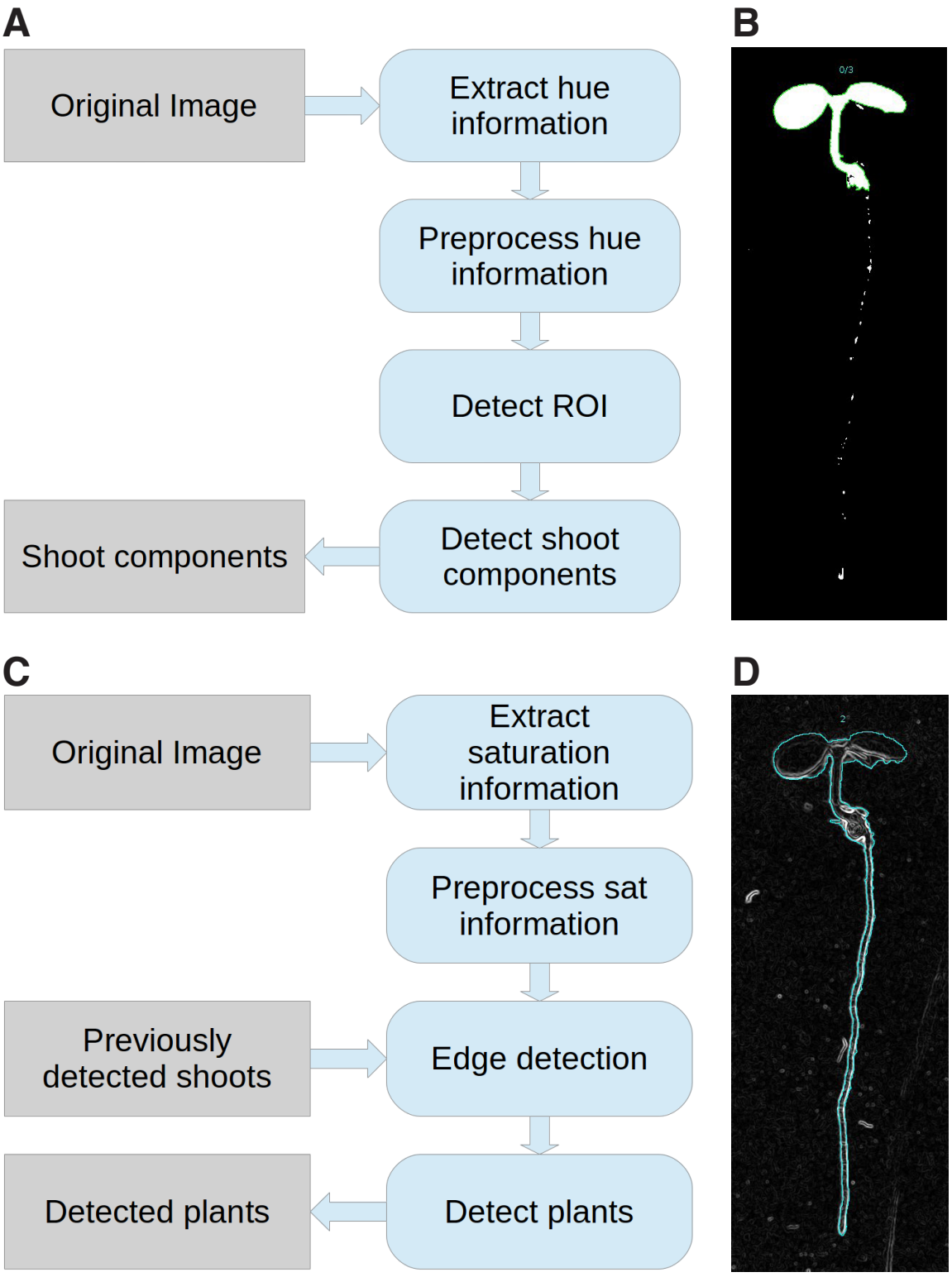

Supplemental Figure 2. Plant and shoot detection algorithms of BRAT

(A) The schematic of the shoot detection algorithm.
(B) A typical result of the shoot detection shown as binary (black/white) representation produced by the algorithm. The detected shoot parts are marked with a green outline.
(C) Schematic of the plant detection algorithm.
(D) A typical result of the plant detection. The outline of the detected plant is shown in cyan.

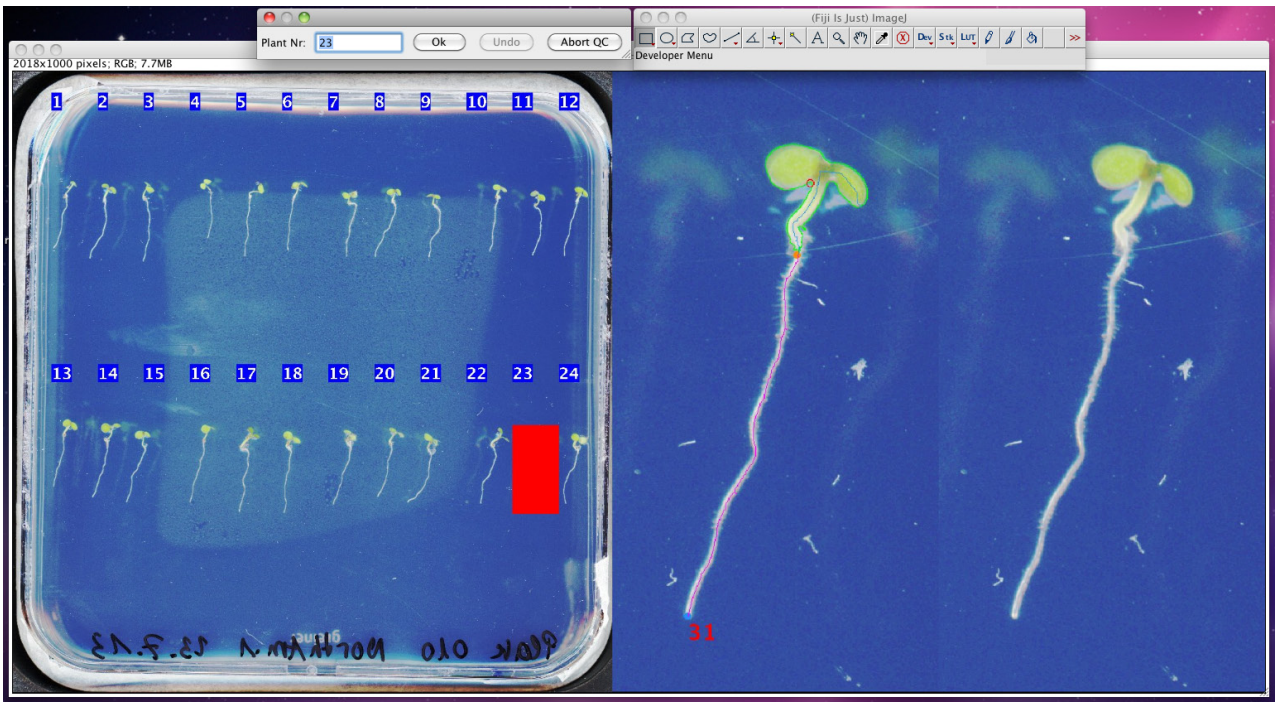

Supplemental Figure 3. Screenshot of the optional BRAT quality control interface

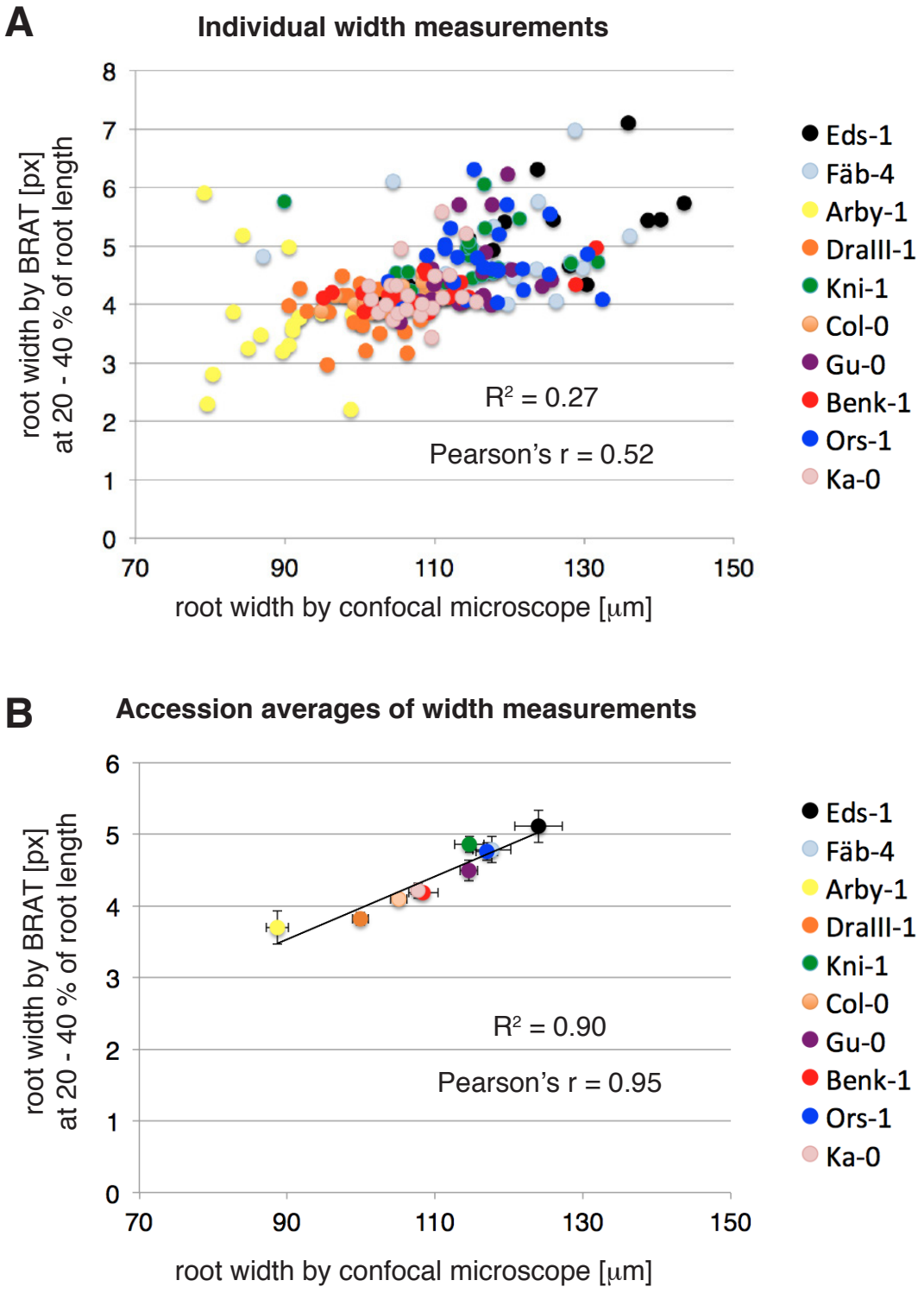

Supplemental Figure 4.
Correlation of root width measurements: BRAT vs. confocal microscopy

(A) Correlation of root width measurements of individual plants of ten accessions using measurements from BRAT (y-axis) and confocal microscopy (x-axis) in the longitudinal interval of 20-40% of root length starting from the hypocotyl/root boundary. Confocal measures are three point averages calculated from width measurements at 20, 30 and 40% of root length. BRAT root width 40 measurements correspond to average of root width at 20 - 40% of root length.
(B) Accession averages and standard error of the mean for data shown in **(A)**.

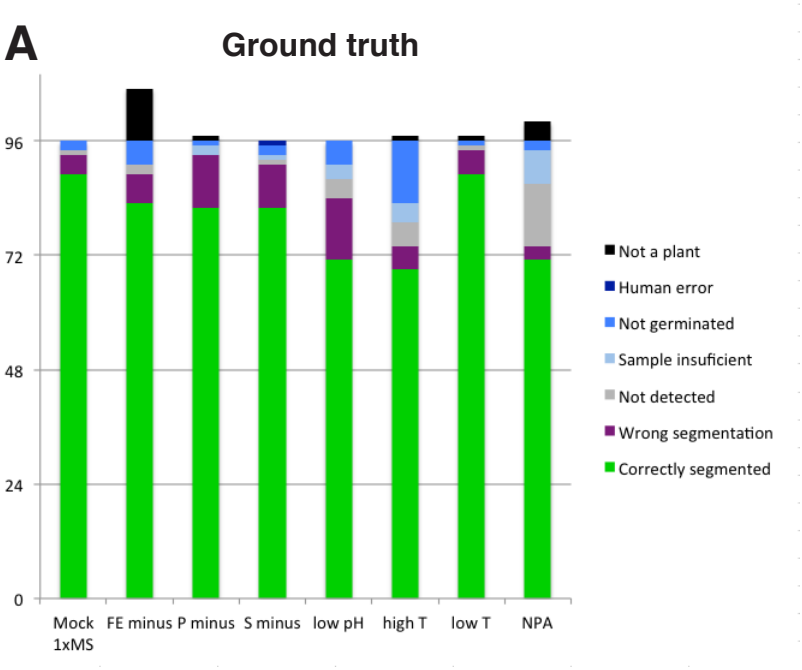

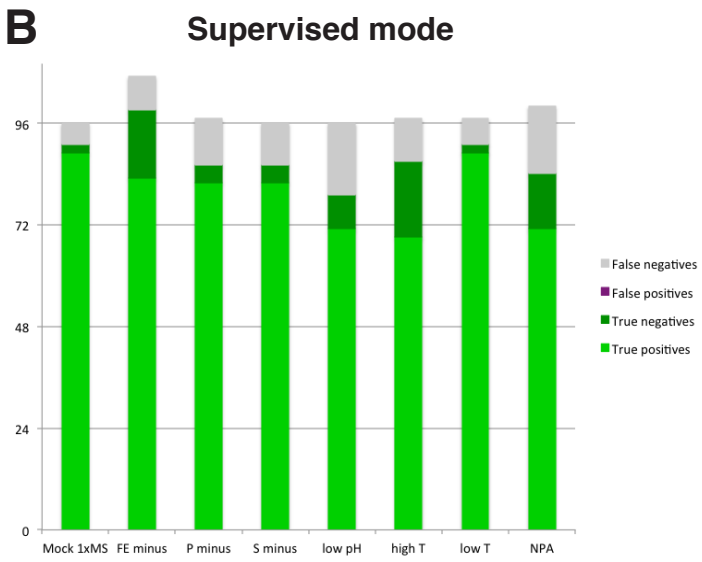

FNR	0.05	0.09	0.12	0.11	0.19	0.13	0.06	0.18
Recall	0.95	0.91	0.88	0.89	0.81	0.87	0.94	0.82

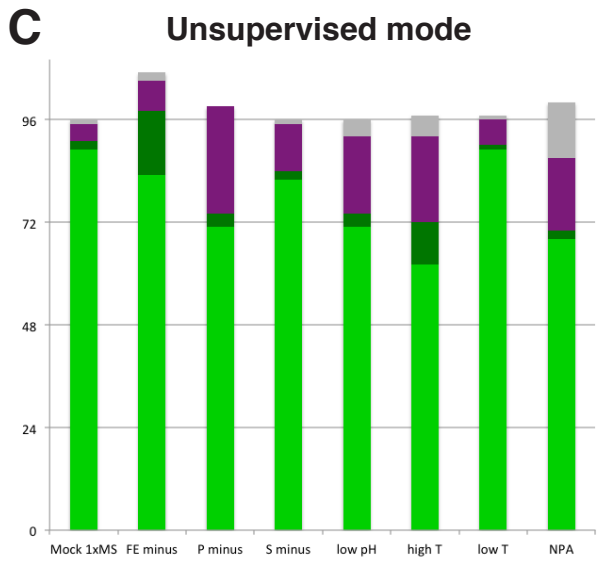

FNR	0.01	0.02	0.00	0.01	0.05	0.07	0.01	0.16
Recall	0.99	0.98	1.00	0.99	0.95	0.93	0.99	0.84
Precision	0.96	0.92	0.74	0.88	0.80	0.76	0.94	0.80
FPR	0.04	0.08	0.26	0.12	0.20	0.24	0.06	0.20

Supplemental Figure 5.
Performance of BRAT under various experimental conditions

(A) Classes of objects after the image segmentation prior to optional validation step.
(B) BRAT output, false negative rates under supervised user scenario.
(C) BRAT output, false negative and false positive rates in unsupervised mode.

A

Accession	Ct-1	Gu-0	Hov4-1	En-1	Brö1-6
Exemplary root images day2 day3	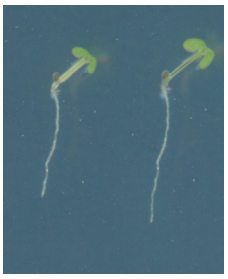	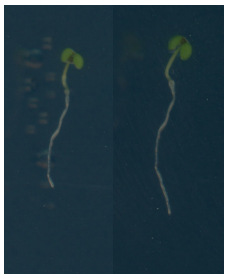		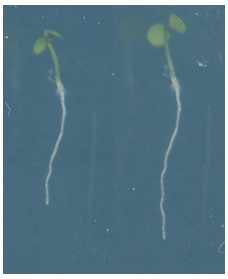	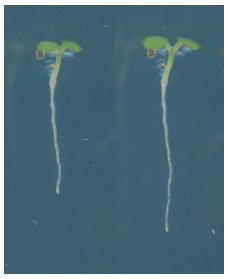
Primary root length (day 2) [mm]	7.1	9.5	10.6	7.5	7.4
Root growth rate (day 2 - 3) [mm/day]	2.2	2.6	3.6	2.9	2.7
Relative root growth rate (day 2 - 3) [% growth]	0.31	0.27	0.34	0.38	0.36

B

Accession	Ba-1	Nok-3	HR-5	N13	Hau-0
Exemplary root images day2 day3	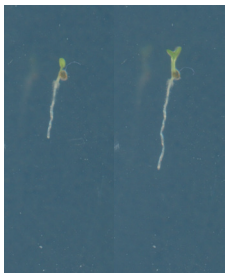	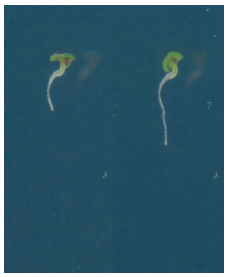	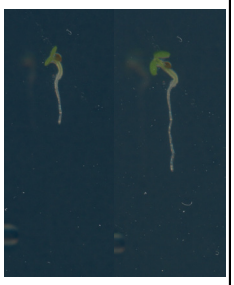		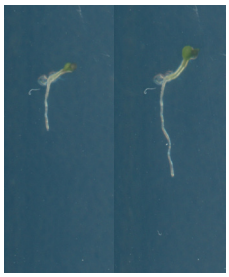
Primary root length (day 2) [mm]	3.1	2.7	2.9	2.3	2.8
Root growth rate (day 2 - 3) [mm/day]	2.3	2.3	2.9	2.2	3.5
Relative root growth rate (day 2 - 3) [% growth]	0.75	0.86	0.99	0.98	1.25

Supplemental Figure 6. Example images of the roots and trait values for extreme accessions for relative root growth rate

(A) Examples of extreme accessions with slow relative root growth rate
(B) Examples of extreme accessions with fast relative root growth rate

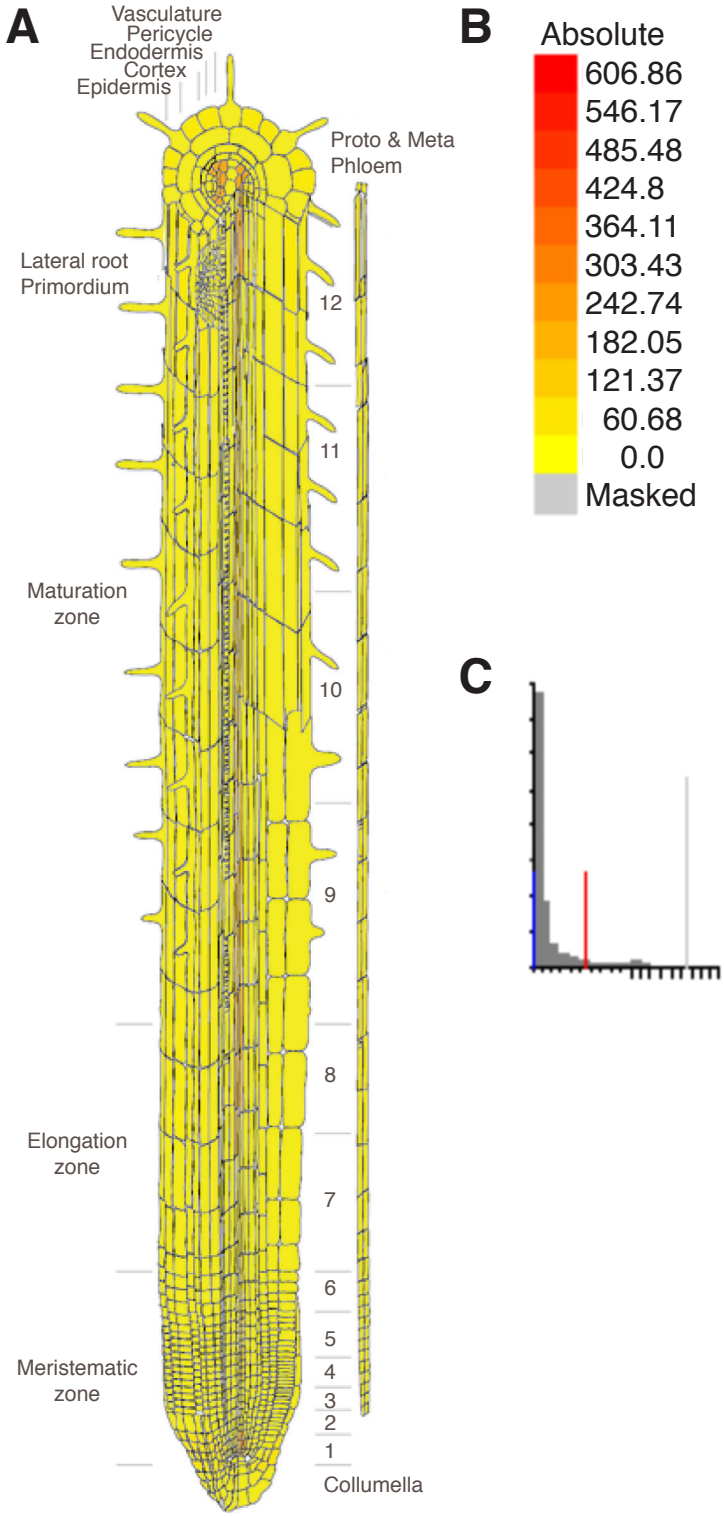

Supplemental Figure 7. Abundance of *CaS* (AT5G23060) transcript in the root

(A) Spatiotemporal map of expression of AT5G23060 in the root; obtained from eFP browser (Brady et al., 2007; Winter et al., 2007).
(B) Color scale depicts expression level in tissue.
(C) Histogram of average expression level of all genes in root data set. Red line in histogram indicates maximum expression of AT5G23060.

Brady, S.M., Orlando, D.A., Lee, J.Y., Wang, J.Y., Koch, J., Dinneny, J.R., Mace, D., Ohler, U., and Benfey, P.N. (2007). A high-resolution root spatiotemporal map reveals dominant expression patterns. SCIENCE **318**, 801-806.

Winter, D., Vinegar, B., Nahal, B., Ammar, R., Wilson, G.V., and Provart, N.J. (2007). An "Electronic Fluorescent Pictograph" Browser for Exploring and Analyzing Large-Scale Biological Data Sets. PLoS ONE **2(8)**, e718.

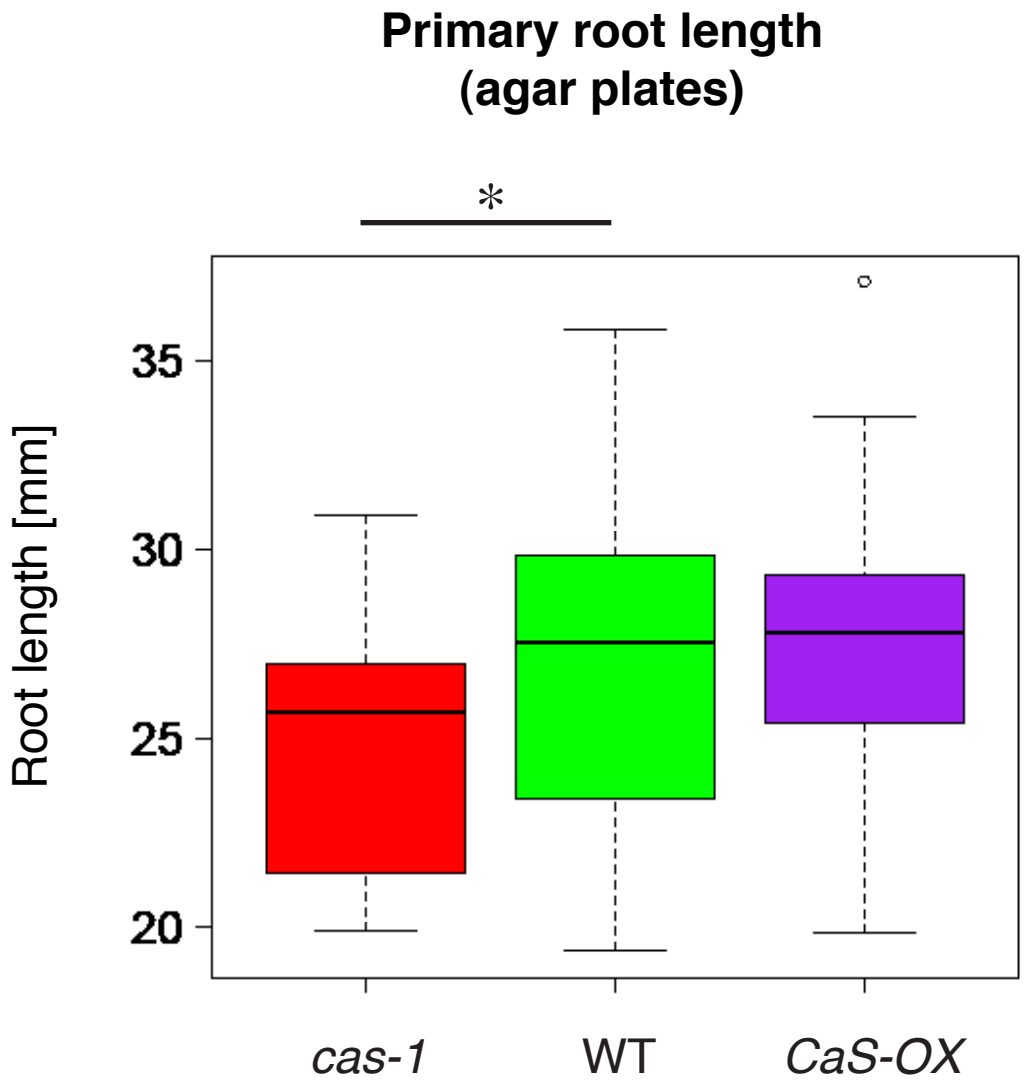

Supplemental Figure 8. Effects of loss of function and overexpression of *CaS* gene on primary root length on agar plates

Boxplot showing primary root length on day 7 after germination in loss of function and 35S overexpression lines of the *CaS* gene (N > 29); x-axis: genotype; y-axis: primary root length [mm]; whiskers: ± 1.5 times the interquartile range (IQR); Student's t-test p-value = 0.013 indicated by: (*).

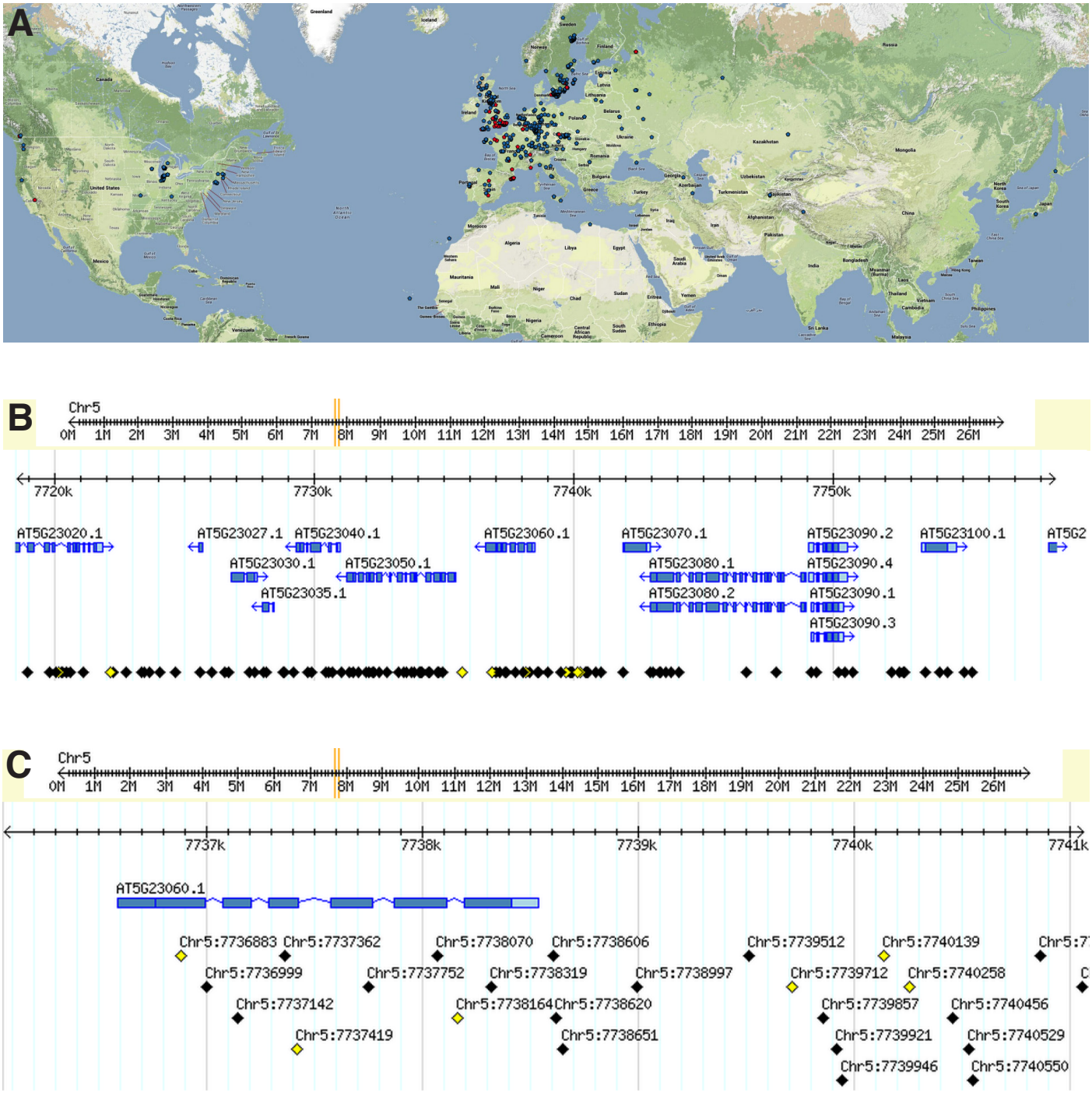

Supplemental Figure 9. Worldwide distribution of alleles for top *CaS* SNP and signs of selection at the *CaS* genomic locus

(A) Geographic distribution of the top *CaS* SNP alleles in 1307 accessions from the RegMap panel (Horton *et al.*, 2012) in the northern hemisphere. *CaS* major alleles at the chromosome 5 position 7738620 (T) are depicted as blue stars, whereas minor alleles (A) are depicted as red stars.
(B), (C) Signs of possible selection in *CaS* genomic locus (F_{ST} p-value < 0.01 shown as yellow diamonds; Horton *et al.,* 2012), screenshots from http://regmap.uchicago.edu/cgi-bin/gbrowse/arabidopsis/; 40 kB window centered on *CaS* gene (AT5G23060) **(B)** and enlarged view for *CaS* genomic locus **(C)**.

Horton, M.W., Hancock, A.M., Huang, Y.S., Toomajian, C., Atwell, S., Auton, A., Muliyati, N.W., Platt, A., Sperone, F.G., Vilhjalmsson, B.J., Nordborg, M., Borevitz, J.O., and Bergelson, J. (2012). Genome-wide patterns of genetic variation in worldwide Arabidopsis thaliana accessions from the RegMap panel. Nat Genet 44, 212-216.

A

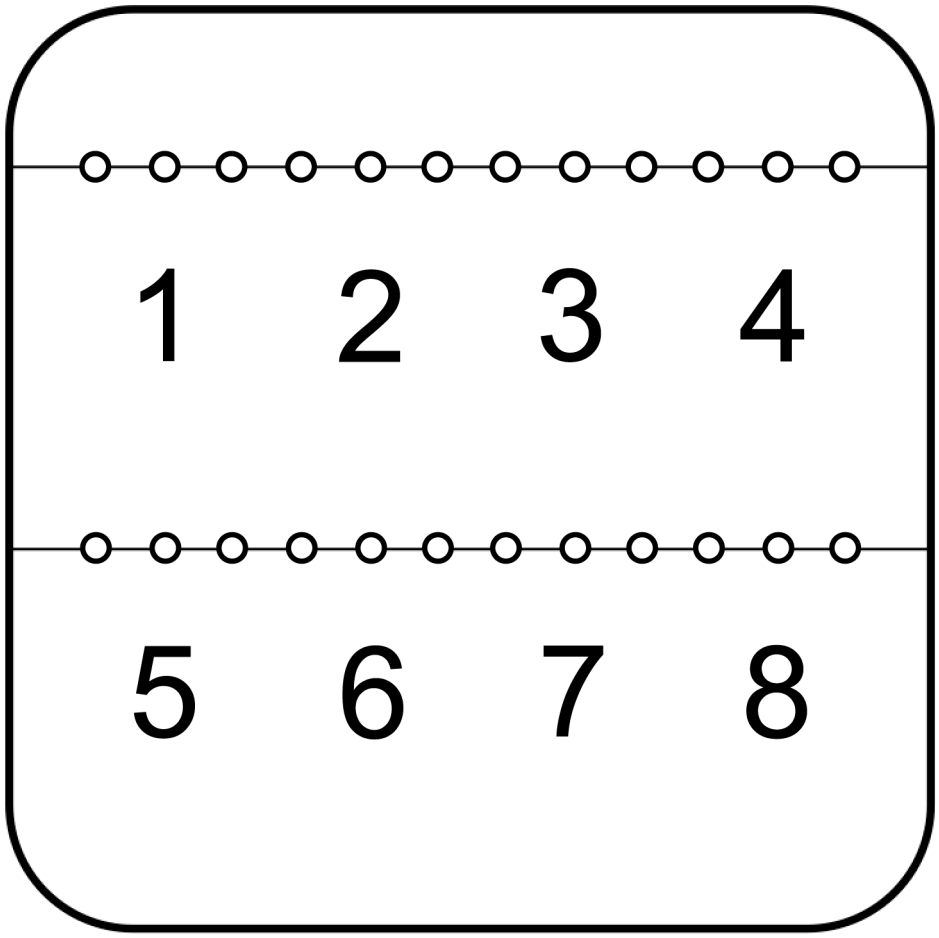

B

plates \ sections	1	2	3	4	5	6	7	8
1	A A A	B B B	C C C	D D D	E E E	F F F	G G G	H H H
2	H H H	A A A	B B B	C C C	D D D	E E E	F F F	G G G
3	G G G	H H H	A A A	B B B	C C C	D D D	E E E	F F F
4	F F F	G G G	H H H	A A A	B B B	C C C	D D D	E E E
5	E E E	F F F	G G G	H H H	A A A	B B B	C C C	D D D
6	D D D	E E E	F F F	G G G	H H H	A A A	B B B	C C C
7	C C C	D D D	E E E	F F F	G G G	H H H	A A A	B B B
8	B B B	C C C	D D D	E E E	F F F	G G G	H H H	A A A

Supplemental Figure 10. Grid layout template and positional permutations

(A) Grid is placed under the plate to guide the biologist to precise placement of the seeds on the agar medium surface. Multiple genotypes can be used per one plate (e.g. eight with three replicates on this template). **(B)** Permutated block design was used to account for positional effects within and between Petri dishes. Schematic of the permutations for three replicates from each of eight accession on eight plates.

A

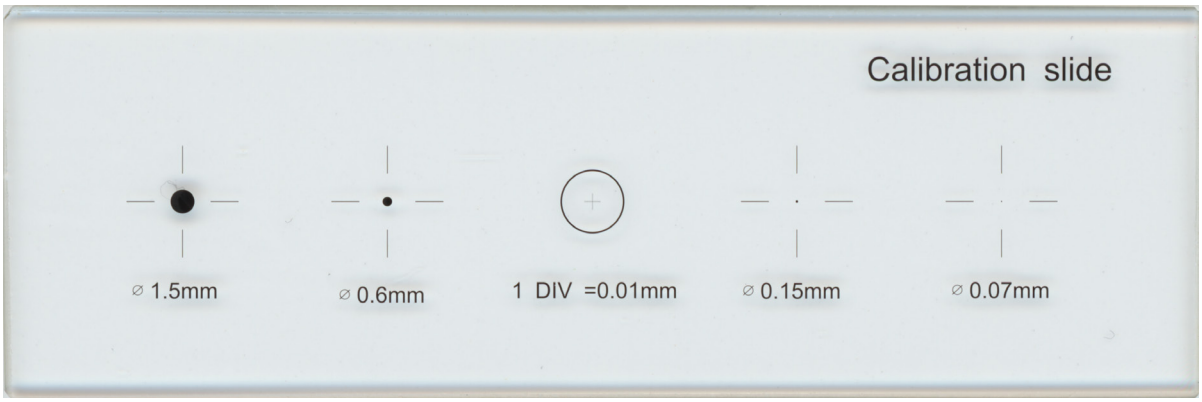

B

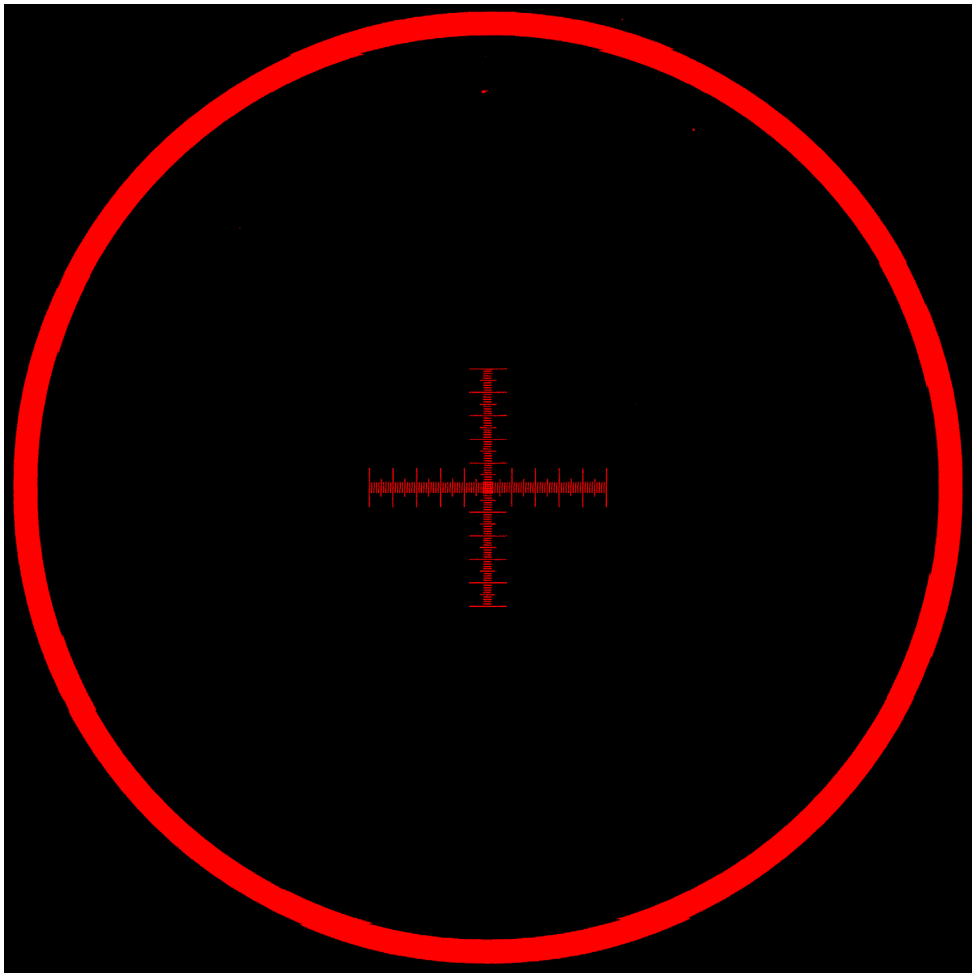

Supplemental Figure 11. Microscope calibration slide

(A) Calibration slide scanned by the scanners used for image-acquisition.
(B) 10 µm scale imaged with Zeiss LSM 700 confocal microscope. The 10µm scale was used to estimate the scanners maximal real resolution to be 50 µm.

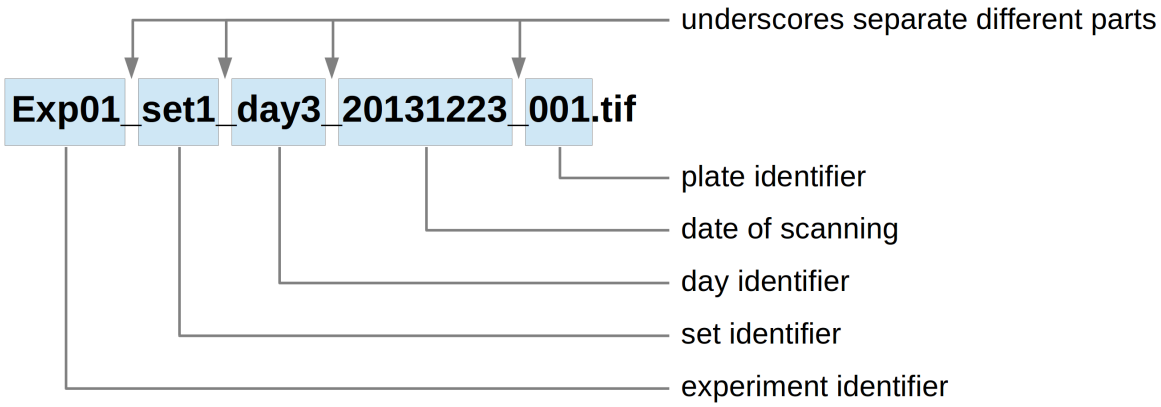

Supplemental Figure 12. The naming pattern supported by BRAT

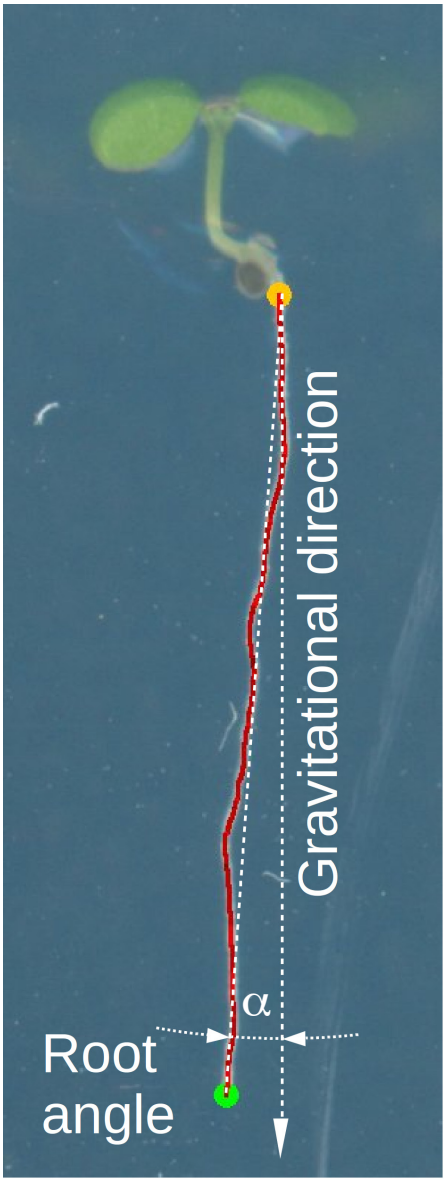

Supplemental Figure 13. Illustration of root angle trait

The root angle describes the angle between the root vector (the line through the root's start and end point) and the y-axis (assumed vector of gravity).

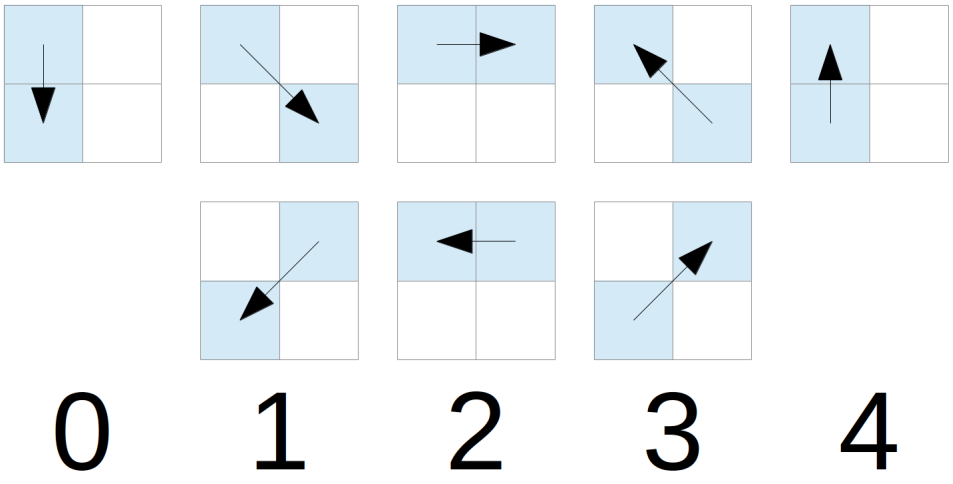

Supplemental Figure 14. Calculation of root direction index

For calculating the “root directional equivalent” we follow the path of the skeletonized main root from start point to end point. Each time we move from one pixel to the next a certain value (according to the scheme in the figure) gets added. For example, if we move straight downwards a value of 0 is added, in case of diagonal downwards direction, the value will be 1. The total sum is then divided by the number of pixels visited. The more gravitropic the root grows the lower the value, the less gravitropic the root grows, the higher the value.

set_nr.	plate_nr.	plate_id	acc_id	row	column
1	1	1	genotype-1	1	1
1	1	1	genotype-1	1	2
1	1	1	genotype-1	1	3
1	1	1	genotype-2	1	4
1	1	1	genotype-2	1	5
1	1	1	genotype-2	1	6
1	1	1	genotype-3	1	7
1	1	1	genotype-3	1	8
1	1	1	genotype-3	1	9
1	1	1	genotype-4	1	10
1	1	1	genotype-4	1	11
1	1	1	genotype-4	1	12
1	1	1	genotype-5	2	1
1	1	1	genotype-5	2	2
1	1	1	genotype-5	2	3
1	1	1	genotype-6	2	4
1	1	1	genotype-6	2	5
1	1	1	genotype-6	2	6
1	1	1	genotype-7	2	7
1	1	1	genotype-7	2	8
1	1	1	genotype-7	2	9
1	1	1	genotype-8	2	10
1	1	1	genotype-8	2	11
1	1	1	genotype-8	2	12

Supplemental Table 1. Genotype layout file

Short exemplary genotype layout text file for one plate containing three replicates for each of eight different genotypes (in total 24 plants in two rows).

	EZ-Rhizo (Armengaud *et al.*, 2009)	RootReader2D (Clark *et al.*, 2013)	SmartRoot (Lobet *et al.*, 2011)	RootTrace (French *et al.*, 2009)	BRAT desktop QC: manual	BRAT cluster QC: manual	BRAT desktop QC: automated	BRAT cluster QC: automated
Image segmentation	53.18 min (27.04 s/root)	40.85 min (20.78 s / root)	30.95 min (15.74 s / root)	11.72 min (5.96 s / root)	3.97 min (2.02 s / root)	2 min (one image on one cluster node)	3.97 min (2.02 s / root)	2 min (one image on one cluster node)
Tested on	Intel Core 7 @ 2.8 GHz; 3 GB RAM assigned to WIN XP virtual machine	Intel Core 5 CPU 650 @ 3.20 GHz; 4 GB RAM WIN 7	Intel Core 5 CPU 650 @ 3.20 GHz; 4 GB RAM WIN 7	Intel Core 5 CPU 650 @ 3.20 GHz; 4 GB RAM WIN 7	Intel Core 5 CPU 650 @ 3.20 GHz; 4 GB RAM WIN 7	Intel Xeon CPU E5520 @ 2.27GHz; 12 GB RAM (node on cluster)	Intel Core 5 CPU 650 @ 3.20 GHz; 4 GB RAM WIN 7	Intel Xeon CPU E5520 @ 2.27GHz; 12 GB RAM (node on cluster)
Quality control mode	validation step intrinsic	validation step intrinsic	validation step intrinsic	not supported	optional validation manual:	optional validation manual:	optional validation automated:	optional validation automated:
QC time requirements	included in image segmentation	included in image segmentation	included in image segmentation	not supported	7.6 min (3.87 s / root)	7.6 min (3.87 s / root)	one time: 1.0 min	one time: 1.0 min
Estimated time for 19 560 roots	147 hours	113 hours	86 hours	32.4 hours	32.0 hours (11 + 21 hours)	21 hours (2 min + 21 hours)	11 hours (11 hours + 1 min)	3 min (2 min + 1 min)
QC tested on	same as above	same as above	same as above	not supported	Intel Core 5 CPU 650 @ 3.20 GHz; 4 GB RAM WIN 7	Intel Core 5 CPU 650 @ 3.20 GHz; 4 GB RAM WIN 7	Intel Core 5 CPU 650 @ 3.20 GHz; 4 GB RAM WIN 7	Intel Core 5 CPU 650 @ 3.20 GHz; 4 GB RAM WIN 7
Image size	6.4 MB	397 KB	8.5 MB	700 KB	25.7 MB	25.7 MB	25.7 MB	25.7 MB
Image resolution	300 dpi	300 dpi	600 dpi	600 dpi	600 dpi*	600 dpi*	600 dpi*	600 dpi*
Image type	RGB .bmp	RGB .jpg	greyscale .tif	RGB .jpg	RGB .tif	RGB .tif	RGB .tif	RGB .tif

Supplemental Table 2.
Time requirements of high-throughput root phenotyping software

Performance evaluation was based on the same 5 images of plates containing in total 118 plants. Image formates and resolution were chosen according to software specifications and to allow for good performance of the evaluated software.
(*) these images were downsampled to allow comparison with other software.

Armengaud, P., Zambaux, K., Hills, A., Sulpice, R., Pattison, R.J., Blatt, M.R., and Amtmann, A. (2009). EZ-Rhizo: integrated software for the fast and accurate measurement of root system architecture. PLANT JOURNAL 57, 945-956.

Clark, R.T., Famoso, A.N., Zhao, K., Shaff, J.E., Craft, E.J., Bustamante, C.D., McCouch, S.R., Aneshansley, D.J., and Kochian, L.V. (2013). High-throughput two-dimensional root system phenotyping platform facilitates genetic analysis of root growth and development. Plant Cell Environ 36, 454-466.

Lobet, G., Pages, L., and Draye, X. (2011). A novel image-analysis toolbox enabling quantitative analysis of root system architecture. Plant Physiol 157, 29-39.

French, A., Ubeda-Tomas, S., Holman, T.J., Bennett, M.J., and Pridmore, T. (2009). High-throughput quantification of root growth using a novel image-analysis tool. Plant Physiol 150, 1784-1795.

Name	Origin	GWAS ID	Name	Origin	GWAS ID
Aa-0	GER	7000	**Ct-1**	ITA	6910
Ak-1	GER	6987	**CUR-8**	FRA	86
Algutsrum	SWE	8230	**Cvi-0**	CPV	6911
Amel-1	NLD	6990	**Da-0**	GER	7094
An-1	BEL	6898	**Dem-4**	USA	8233
Ang-0	BEL	6992	**Di-1**	FRA	7098
Arby-1	SWE	6998	**Do-0**	GER	7102
Ba-1	UK	7014	**DraII-1**	CZE	8284
Bå1-2	SWE	8256	**DraIII-1**	CZE	8285
Bå4-1	SWE	8258	**Duk**	CZE	6008
Bå5-1	SWE	8259	**Eden-2**	SWE	6913
Baa-1	NLD	7002	**Edinburgh-5**	UK	9302
Bay-0	GER	6899	**Eds-1**	SWE	6016
Bch-1	GER	7028	**Ei-2**	GER	6915
Benk-1	NLD	7008	**EM-183**	UK	461
Bla-1	ESP	7015	**Ema-1**	UK	5736
Boot-1	UK	7026	**En-1**	GER	8290
Bor-1	CZE	5837	**Ep-0**	GER	7123
Bor-4	CZE	6903	**Es-0**	FIN	7126
Br-0	CZE	6904	**Est-1**	RUS	6916
Brö1-6	SWE	8231	**Fäb-4**	SWE	6918
Bs-1	SUI	8270	**Fei-0**	POR	8215
Bs-2	SUI	7004	**FOR-5**	UK	936
Bsch-0	GER	7031	**Frd-1**	UK	5742
Bu-0	GER	8271	**Ga-0**	GER	6919
Bur-0	IRL	5719	**Gd-1**	GER	8296
C24	POR	6906	**Ge-0**	SUI	8297
Ca-0	GER	7062	**Gel-1**	NLD	7143
Cala-8	ESP	9152	**Gie-0**	GER	7147
Can-0	ESP	8274	**Got-22**	GER	6920
Chat-1	FRA	7071	**Got-7**	GER	6921
Chr-1	UK	5723	**Gr-1**	AUT	8300
CIBC-17	UK	6907	**Gu-0**	GER	6922
CIBC-5	UK	6730	**Gy-0**	FRA	8214
Cit-0	FRA	7075	**Ha-0**	GER	7163
Co	POR	7081	**Hau-0**	DEK	7164
Coc-1	ESP	5729	**Hey-1**	NLD	7166
Col-0	USA	6909	**Hh-0**	GER	7169
Com-1	FRA	7092	**Hi-0**	NLD	8304
Crl-1	UK	5731	**Hil-1**	UK	5745

Name	Origin	GWAS ID	Name	Origin	GWAS ID
HSm	CZE	8236	**Lo-2**	GER	7242
In-0	AUT	8311	**Lp2-6**	CZE	7521
Is-0	GER	8312	**Map-42**	USA	2057
Je-0	GER	7181	**Mc-0**	UK	7252
Jl-3	CZE	7424	**Mdn-1**	USA	1829
Hl-3	GER	7172	**MNF-Pot-80**	USA	1874
Hov4-1	SWE	8306	**Mr-0**	ITA	7522
HR-10	UK	6923	**Mrk-0**	GER	6937
HR-5	UK	6924	**N13**	RUS	7438
Hs-0	GER	8310	**Nok-3**	NLD	6945
Jm-0	CZE	8313	**Nyl-2**	SWE	6064
Jm-1	CZE	7178	**ÖMö2-3**	SWE	7519
Ka-0	AUT	8314	**Ör-1**	SWE	6074
Kelsterbach-4	GER	8420	**Ors-1**	ROM	7283
Ker-38	USA	1782	**Ost-0**	SWE	8351
Kil-0	UK	7192	**Pa-1**	ITA	8353
Kin-0	USA	6926	**Pent-1**	USA	2187
Kl-5	GER	7199	**Pna-10**	USA	7526
Kni-1	SWE	6040	**Pna-17**	USA	7523
Kno-10	USA	6927	**Pro-0**	ESP	8213
Kno-18	USA	6928	**Rak-2**	CZE	8365
Köln	GER	8239	**Rev-1**	SWE	8369
Kondara	TJK	6929	**Rhen-1**	NLD	7316
Kr-0	GER	7201	**Rmx-A02**	USA	7524
Krot-2	GER	7205	**RRS-10**	USA	7515
Kulturen-1	SWE	8240	**RRS-7**	USA	7514
Kyl-1	UK	5751	**San-2**	SWE	8247
Kz-1	KAZ	6930	**Sanna-2**	SWE	8376
Kz-9	KAZ	6931	**Spr1-6**	SWE	6965
La-1	GER	7210	**Tamm-2**	FIN	6968
LAC-5	LAC	96	**Tamm-27**	FIN	6969
Lag1-6	GEO	9104	**Ting-1**	SWE	7354
Lan-1	UK	5752	**Tiv-1**	ITA	7355
Lc-0	UK	8323	**TOU-J-3**	FRA	383
LDV-58	FRA	149	**Ts-5**	ESP	6971
Ler-1	GER	6932	**Uod-7**	AUT	6976
Li-3	GER	7224	**Vår2-1**	SWE	7516
Li-7	GER	7231	**Ven-1**	NLD	7384
Liarum	SWE	8241	**Vimmerby**	SWE	8249
Lip-0	POL	8325	**Ws-2**	RUS	6981
LL-0	ESP	6933	**Yo-0**	USA	6983
Lm-2	FRA	8329			

Supplemental Table 3. 163 accessions used in this study